

The restitution coefficient value and damage of composite shields protecting the chassis of a rail vehicle

Mateusz Juzun¹, Mariusz Pawlak^{2*} 

¹ Silesian University of Technology, ul. Akademicka 2A, 44-100 Gliwice, Poland

² Capgemini, ul. Żelazna 2-4, 40-851 Katowice, Poland

* Corresponding author's e-mail: mariusz.pawlak@polsl.pl

ABSTRACT

To protect the undercarriage of a railway vehicle moving at high speeds, rolling stock manufacturers use shields made of polymer composites. During operations, damage to these guards is often observed due to railway ballast hitting them. Verification of the course of the impact and the extent of damage caused to these shields has drawn attention to the potential effect of the structural damping of the material on the impact resistance of these shields. This property is expressed by the coefficient of restitution, which determines the amount of energy absorbed by the material during the impact, and its direct influence on the simulation results is rarely a separate research subject. In this paper, an attempt was made to verify the influence of this coefficient on the compliance of railway ballast impact simulation results with the results of bench tests. Two test stand were built for this purpose: to measure the coefficient of restitution of the composite samples and to verify the impact resistance of shields. The principle of the restitution coefficient tester is based on the ISO 10545-5 standard and its operation is based on measuring the time elapsed between two consecutive impacts of a steel ball on the surface of the tested specimen. The experimental tests carried out led to the determination of the coefficient for the composite material adopted. This material was a laminate of flax fibres and epoxy resin with a core of 2 different types of materials, i.e., XPS and EPS, and the coefficient values obtained were 0.74 and 0.69 respectively. Knowing these values allowed us to relate the extent of damage caused to the value of the restitution coefficient. To simulate the impact of the railway ballast on the casing, a second test bench was prepared, which allowed the impact to be reproduced. The observed significant effect of restitution coefficient on the results confirmed the validity of the assumption.

Keywords: restitution coefficient, impact, damage, chassis rail.

INTRODUCTION

Due to the increasing speed of rail vehicles travelling on rail routes, there is an increasing risk of the number and severity of the impacts of stones forming the track superstructure on the chassis surface. This phenomenon leads to numerous damages during the operation of the vehicles. Therefore, in order to protect the chassis against the effects of impacts, dedicated protective shields are used to protect the structure and the installed equipment. The guards are made from a variety of materials, but due to the dynamic development of the composites industry, polymer composites have been used for this purpose for many years. This is due to the

numerous advantages that this material offers over metals. These include lower weight, high mechanical strength and rigidity. Composite materials are also characterised by the possibility to manipulate the parameters of the designed component depending on the amount, layout and type of reinforcement used for particular layers. The use of composite materials in chassis protection is an important challenge for the designers of composite casings. Composite materials take complicated forms of mechanical damage compared to metals and their features.

The significance of the problem related to damage to undercarriages is confirmed by operational experience in transport companies, which shows frequent cases of damage to the undercarriages of vehicles

operated on rail routes all over the world. This problem is due to insufficient strength of casings. The attention has been focused on selected, required properties, which the shield should have in order to effectively protect the chassis. The performed bench and numerical tests allowed to select the features that should be considered in the design process in order to obtain a product of high exploitation utility.

Contemporary literature is rich in analyses of composite materials and their resistance to mechanical damage. Apart from the resistance to static loads, which is not the subject of this study, there is a large group of publications dealing with the resistance of composite materials to basic impact. In this type of analysis, the case of high velocity firing of a projectile with a cone end perpendicular to the specimen is considered [1–4]. This type of research is aimed at verifying the applicability of various composite materials, including hybrid materials, as specific bulletproof materials. The work focuses on discussing the following research problems: the influence of the number of layers and type of reinforcement on the resistance, the influence of the material of particular layers on the results, the compatibility of the research results with the results of numerical simulations and the possibility of their application to simulations of other cases.

Another numerous groups of publications deals with the issue of low-energy impacts on composite parts [5–7], and the relevance of this problem has been described as comparable to fatigue tests of composite materials [8]. Low-energy tests focus mainly on impacts of components with relatively smooth shape, low mass and low velocity. Such impacts cause mainly damage inside the structure - delamination, hence they are particularly dangerous, as they are not visible from the outside. Such situations may arise for example from an impact of a falling tool released by a worker during aircraft servicing or from hail falling on an airframe.

The availability of publications describing research on the specific type of impacts discussed in this article is different. Few publications dealing with the issue of resistance of composite casings protecting the chassis of rail vehicles have been found: [9–13]. However, despite the fact that the issue concerns impacts at a low angle to the surface of the specimen, all found publications simplify the tests to impacts directed perpendicularly to the surface. Hence it can be concluded that this information does not provide sufficient basis for making proper design and construction assumptions for the shield constructors.

The state of knowledge in the field of research, topicality of the issues discussed in the paper and lack of research conducted in the context of the discussed type of impacts in the literature prompted the author to analyse this issue and publish the results. Some of the research results were presented in publications [14–15] and at a thematic conference on the application of composite materials [16].

For the majority of modern rail vehicles, and especially electrical multiple units, space is a problem for fitting the equipment on the train. Depending on the permissible running speeds and the type of traffic to be handled, the main areas for fitting equipment include the roof and the chassis. This equipment includes electrical boxes, compressors, reservoirs, piping and electrical wiring and valves. All components mounted on the underbody of a vehicle running on a loose track are subject to erosive impact from stones, also known as ballast. The chassis area of an unprotected vehicle can be damaged and the many nooks and crannies that can collect ice or dust.

Negative effects of impacts may be prevented by a special construction of the vehicle, which excludes the chassis area from installation of any equipment, which is especially the case with vehicles designed for operation in difficult climatic conditions, e.g. in Norway. In this case, solutions ensuring simplicity of the mentioned area and lack of equipment in this zone are introduced already at the design and construction stage. However, this complicates the vehicle structure and generates high costs.

This solution is not common, and the chassis of other vehicles can be secured in a different way. For this purpose, especially in the case of high-speed rail vehicles, special shields screwed onto the chassis are used [17]. These covers provide a uniform surface when installed and cover the pipes and cables running under the floor. To improve the effectiveness of the protection, their shape in cross-section to the wagon axis is gently rounded upwards. Fig. 1 shows an example of a chassis protected by bolt-on protective covers. The installation method and shape of these guards also guarantees an improvement in the train's aerodynamic performance. It is also important that the chassis is easier to keep clean during normal operation, but also when clearing up after railway incidents.

For accessibility and ease of use, the guards are divided into sections, dimensionally adapted to the area to be protected.

In addition to the above-mentioned features, the use of casings in passenger trains contributes to acoustic insulation, affecting passenger comfort.



Figure 1. Chassis of a railway vehicle equipped with protective guards

Each casing is peripherally equipped with gaskets which, when compressed by tightening them to the chassis structure, acoustically isolate the space from external factors. Shields itself may also have properties improving acoustic insulation in case it is built of polymer composites, especially with sandwich structure [18,19]. Noise sources in the wagon interior can be either stones hitting the chassis or air.

In addition, the use of perimeter seals limits the ingress of water, snow and dust into the chassis compartment, where more weather-sensitive components may then be built in. At the same time, the thermal insulation of the passenger compartment from ambient conditions is ensured. This contributes to the savings associated with reduced heating, cooling and heat loss in the passenger compartment.

Metal plate or composite sandwich structures are most commonly used to construct the shields. However, composite materials have the advantage of better vibration isolation performance and low weight, which is why a polymer composite sandwich structure is used in most new vehicles.

However, its use requires an awareness of the influence of individual plastic properties on impact resistance, hence the importance of carrying out appropriate calculations and simulation studies [15].

CAUSES OF DAMAGE TO VEHICLE CHASSIS RAIL

The analysis of literature exploring the phenomenon of damage to rail vehicle undercarriages during operation has made it possible to note that several causes of damage to the undercarriage can be identified for trains, but the main, direct source of the damage under consideration is the impact caused by the railway ballast forming the track bed. There are two

types of tracks that differ in construction, i.e. ballasted track and slab track [20]. Each of them has its own advantages and disadvantages, whereas in terms of application, ballasted track is used for both normal and high-speed railway, whereas slab track is mainly used for high-speed railway. Both types are equally able to cope with safe operating conditions even at high train speeds. However, it has been noted that slab track requires less maintenance and has a longer service life [21–22]. For cost reasons, ballast-based tracks are very often used, for example, in France, Spain, Italy and Poland. In France, all high-speed railways for which the operating speed exceeds 320 km/h are based on ballast tracks.

A disadvantage of ballasted tracks is the possibility, mentioned at the beginning, of stones rising. This phenomenon has not been fully explained to date, but it is known that it results from a combination of mechanical and aerodynamic forces generated by the passage of a train, which causes some of the stones to overcome the force of gravity and rise up towards the vehicle. These stones cause damage to the heads of rails, train chassis, but also to adjacent structures standing by the tracks, and in extreme cases even injure people in the vicinity [23]. The phenomenon is most dangerous at speeds exceeding 300 km/h, while it is also observed at much lower speeds, below 160 km/h [24–25]. It is similar in the case under consideration in this study, probably caused by additional factors favouring the rise of stones from the ground surface.

The phenomenon of stone trickling affects railway lines worldwide, and more and more railway companies continue to report problems associated with it. The phenomenon of stone chipping is one of the main problems caused by the increase in the speed of rail vehicles, in terms of safety and the deterioration

of vehicles and equipment operating the railway. The causes of the movement of the stones forming the ballast include the above-mentioned combination of mechanical and aerodynamic effects, caused mainly by strong gusts of air, negative pressure and weather conditions, which influence the retention of the ballast.

In extreme weather conditions, foreign objects such as ice fragments may detach from the chassis and cause the stones to move by imparting kinetic energy in the collision process [9]. On the basis of research carried out in winter conditions, it was determined that statistically, on a day with an average temperature of -3 °C and snowfall of 3 cm, lumps of ice settling on the undercarriage can reach a mass of 5–10 kg [27]. When the train is moving at high speeds in a cold climate, ice fragments build up in the vicinity of the wheelsets, forming extended and heavy lumps.

One of the situations considered is the entry of a train into a tunnel, where the ambient temperature may increase causing ice fragments to melt and fall onto the tracks, which may result in uplifting stones. This case applies mainly to operations in countries with cold climates such as Japan, northern Europe or northern China [23]. Another case is when a train, on which ice blocks have deposited, passes through a railway turnout, which causes the vehicle to vibrate, which can result in the blocks being thrown off the train. The phenomenon of ice block detachment has been simulated in experiments carried out, among others, by the French railway company SNCF. In other cases, under conditions of dynamic and aerodynamic interaction through trains moving at high speeds, the stones vibrate, loosening the contact between them and thus reducing the degree

of jamming. This leads to displacement of the loose stones, and when the moving train induces additional aerodynamic effects, this can provide sufficient energy to overcome the gravitational force and lift the stones upwards [23].

This topic is dealt with from the analytical side, among others, by Jing et al [23], who developed a simple equation to detect the key factors of aerodynamic and dynamic effects. The probable occurrence of a ballast lift event may be modelled as a combination of 2 events, i.e. movement of stones from their resting positions, the so-called slackening, and their lifting from the surface.

However, depending on the direction of movement and the initial energy, some of the stones picked up for flight may reach a height allowing them to make contact with the running gear of the passing train. This phenomenon is presented in detail in Fig. 2. As a result of the tests carried out by Kawashima K. et al. in [28], the possible angle Θ of the vector direction of the moving stone in the range from 0° to 70° relative to the longitudinal horizontal axis was determined.

It has been studied that the velocity of a gust of wind caused by a train moving at 300 km/h reaches approx. 25 m/s in the vicinity of the rail head [23]. Assuming that the train in the case under consideration is moving at a maximum speed of 72.2 m/s, the maximum speed of the stone at the start of lift from the track was estimated as 20 m/s. Since only some of the stones carried by the gust reach the undercarriage of the passing vehicle, their speed at the moment preceding the impact is strongly reduced due to transformation of the kinetic energy of the stone with the increase in height into potential energy. Based on this value, it was assumed that at the moment

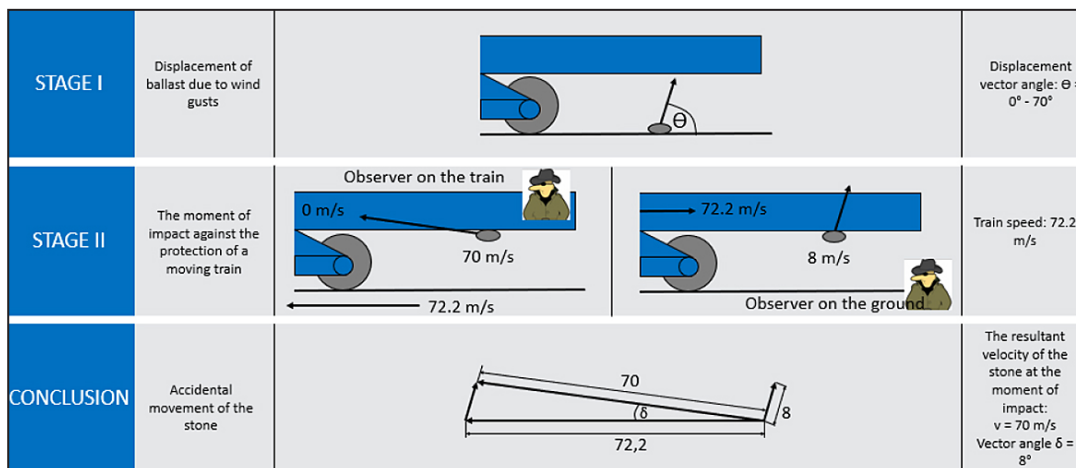


Figure 2. Vector representation of the stone pick-up phenomenon

of impact with the chassis this value does not exceed 8 m/s. Therefore, the main factor influencing the impact parameters is the horizontal speed of the moving train. The distribution of the components can be observed in Figure 2. Taking into account an assumed speed of the moving train of 260 km/h (expressed in Figure 2 as 72.2 m/s), the distribution of vectors was used to determine the impact angle θ of 8° and the accidental impact speed of 252 km/h (expressed in Figure 2 as 70 m/s), which corresponds almost to the speed of the moving train.

To sum up, a case is considered in which the velocity of stone impact against the chassis shall be 252 km/h and the angle of impact shall be 8° to the chassis surface. The mass of the stone, as an impact element, shall be 60 g and be due to the average mass of the ballast which makes up the ballast. The energy of a single stone at the moment before impact is $E_k = 147$ J. It should be emphasised that on the basis of the observation of damage on the chassis of rail vehicles, it was found that the direction of impact of stones is always consistent with the direction of a moving train.

In order to analyse the problem in detail, the railway undertaking was asked to make the damaged shield available for detailed analysis and destructive testing. This made it possible to assess the degree of actual damage caused during operation. The delivered composite shield, presented on Figure 3, was dismantled from an electric multiple unit operating on Polish railway lines. Due to the large external dimensions of the casing, areas of particular interest were first selected and classified, which



Figure 3. A cover from an electric multiple unit withdrawn from service due to multiple erosion damages and perforations. On the right side a detailed view of exemplary damage with dimensions

were then isolated by cutting them out. Based on the analysis of the classified damage, 2 predominant types were distinguished:

- a) regular, repeated, shallow erosion damage, all facing the same direction relative to the direction of vehicle movement.
- b) irregular damage in the form of punctures, resulting from an incidental impact of a rigid element such as a bar, plate or other metal part. In this case, full penetration of the laminate, and sometimes even of the entire composite, occurred.

The methodology proposed in this paper applies only to cases of the type a. This is because type b failures are incidents and, although they lead to the immediate removal of the shield from service, they are not a consequence of operation under normal conditions. The damage analysis carried out with an electron microscope, the effects of which are partly presented in Figure 4, allowed a detailed inspection of the damage area. As a result of the research, the directional character of the damage was confirmed, with well visible zones, such as: matrix layer scraping (zone A and B) and a small amount of “broken” fibres, which may indicate that most of them are removed from the composite during the damage formation, thus increasing the area of destruction [24].

The large amount of fibre removal resulting in erosion loss, is further compounded by the fact that the fibres in the outer layer of this composite are short and randomly distributed in the layer. On the one hand, this brings the strength and stiffness properties in the plane of the layer closer to isotropic, but on the other hand, it does not allow the full use of the possibilities offered by composite materials, which consist in the conscious manipulation of stiffness and strength in particular directions in order to obtain optimal results.

IMPULSE IMPACT VERIFICATION TEST BENCH

According to the literature, the first factor considered is the directionality of anisotropy of the composite layers in relation to the direction of the impact axis. Thanks to the use of polymer composites for the construction of shields, there is a great possibility to manipulate certain features of the finished product in order to optimise the parameters. Therefore, the construction of the reinforcement layer in the form of directional fibres, which have strong anisotropic

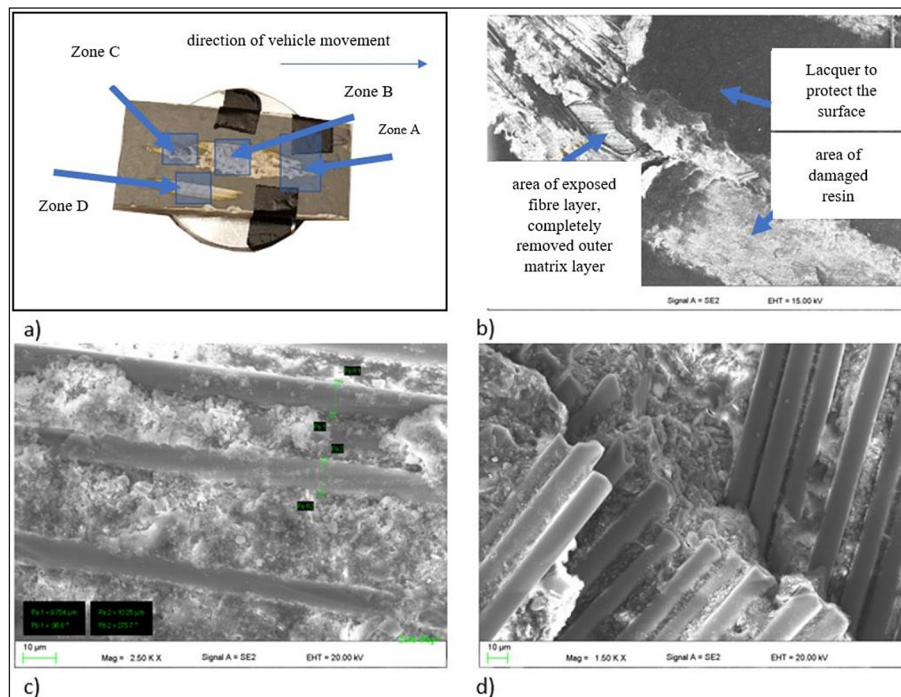


Figure 4. A fragment of a damaged shield under observation. (a) sample prepared for testing (b) Zone A, over 100x (c) Zone B, over 2500x (d) Zone C, over 1500x

properties, was assumed. Taking into account the considered, repeated direction of the impact, it is reasonable to verify the influence of the fibre orientation in the outer layers of the composite on the extent of the damage. The change of fibre arrangement causes the change of direction of the highest stiffness of layers directly exposed to the impacting element.

On the basis of publications [15, 34] the directionality of the fibres forming the outer layer according to the direction of movement of the impacting object should minimise impact area by ensuring that the impactor can slide. For sliding after contact between the impacting object and the composite shield to be possible, it is necessary to minimise the friction coefficient “f”, the value of which influences the formation of tangential impulses affecting the behaviour of the stone at impact. This is the second factor that was taken into account in the experiment. According to the description of the impact mechanics presented earlier, the amount of energy which is dissipated by the shield during the impact is influenced by the damping properties of the material, one of the determinants of which may be the value of the restitution coefficient [30].

This coefficient determines the amount of energy returned to the system depending on the stiffness of the impacted element. Since, in the case of elastic rebound, part of the impact energy is returned to the striking member without increasing the extent of

plastic damage to the striking member, this coefficient of restitution was taken as the third factor to be considered in the preparation of the model and experiment.

Developing a phenomenological model, one should start by presenting the relevance problems for solving the research problem [35]. The task of the model is to reproduce the phenomenon occurring during the impact of sharp-edged elements (stones) on the cover made of a polymer composite material protecting the chassis of a railway vehicle.

In preparing a phenomenological model, the essence of the phenomenon must be reproduced, rejecting or minimising the influence of the physical appearance of the objects under study. This model does not have to refer to the actual geometrical form. The purpose of developing such a model is to prepare the basis for the creation of a numerical model correctly representing the essential features of the phenomenon occurring. For this purpose, it is necessary to make certain assumptions and simplifications.

Due to the lateral dimensions of the train, the composite panel being tested, depending on the variant, has dimensions exceeding 2000×2000 mm. For the purposes of testing, the specimen was minimised and the size of 120×120 mm was adopted as the size that allows mapping the tested phenomenon without significantly affecting the result. This is due to the fact that, in this case, the impact force reaches high values causing high stresses

and deformations located near the impact point. Despite the fact that this place becomes a source of wave propagation covering the whole body volume and transforming into vibrations, these deformations are accompanied by lower material strains than in case of local deformations [7].

The results of the analysis of damage caused by stones on the shield examined in literature allowed the impact to be treated as a local impact, ignoring the effect of the vibration phenomenon mentioned above. As the sample represents only a fragment of the shield, it was assumed that also the shape of the cross-section is simplified. The cowl has in fact a gently rounded shape (the radius of the rounding is $R = 10.000$ mm) in the direction transverse to the longitudinal axis of the vehicle. However, due to the consideration of a small section, it was assumed that the specimen is quite flat.

The composites used to make the shields are layered materials, which are formed from polymer-saturated fibre reinforcements and fillers applied in layers [36] of sandwich structure. It is necessary to model a proper cross-section of the material. The cross-section of the material, which forms the existing casing, is shown in Figure 5. According to the drawing, the casing consists of load-bearing laminate shell layers, and the space between them is filled with a spacer layer made of light material – polyurethane PUR foam. The laminate facings give shape and provide mechanical strength to the casing, while the foam placed between them provides stiffness [15].

In order to represent the impact phenomenon under consideration, particular consideration shall be given to the outer layers directly exposed to contact and impact damage. For this reason the model deliberately omits the geometry of the rear cladding. The mentioned external part of the composite-laminate, is considered on a macroscopic scale, micromechanics issues were not discussed, because the relation on the level of resin-single fibre is not the subject of this research. The macroscopic model was analysed, and the research was conducted in order to estimate and predict the extent, area of damage occurring on the surface [37].

The striking element in real operating conditions are stones, i.e. brittle objects with sharp edges, striking the chassis at high speed [9, 28]. In order to reproduce the impact in a reproducible manner and feasible also under experimental conditions, a sleeve-shaped object with high rigidity was adopted as the impacting element. Since the impact angle $\alpha = 8^\circ$, the impact is made by means of the outer edge. The actual impact energy calculated in analysed example is 147 J, which corresponds to the impact energy presented in the standard [17] for class K8, namely 170 J (Fig. 6).

The analysis of the literature has shown the existence of many different theories and methods allowing verification of the made assumptions concerning the resistance of external layers of the shield to erosive effects of external factors. These include, for example, the single or indentation scratch test (SST) described by Mzali et al. [38], or the

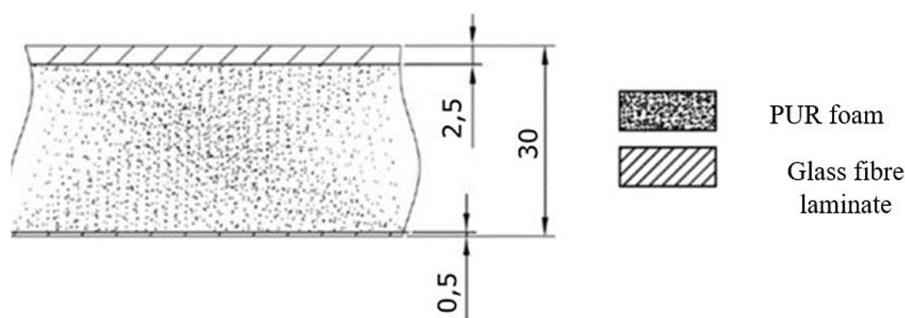


Figure 5. Macroscopic cross-sectional drawing of the existing shield

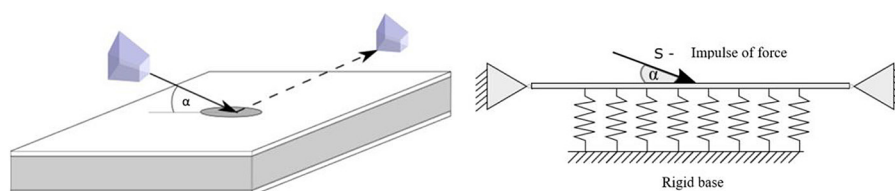


Figure 6. Phenomenological model of the impact process

method described in ISO 20567-1 [39] for testing the resistance of coatings of paints and varnishes by multiple impact tests. Further methods and approaches are described in publications [7, 8, 40]. After the analysis of the field of possible solutions, it was decided in the design process to use the solution based on the guidelines contained in the standard NF F07-101 “Railway applications – simulation shock test ballast projection” [68] while introducing several important modifications.

This standard describes the test of striking a test specimen with an impactor which, due to its initial velocity, has a kinetic energy as required for the relevant impact class. The standard defines impact classes from 12 J to 285 J depending on the energy. The outer profile of the impactor is defined by the standard as a pointed cone, which makes it easy to penetrate the material. The angle of impact is defined as a value between 0° and 350° .

In relation to the guidelines developed in the process of building the phenomenological model, modifications were made to the theory of the study, which included:

- modification of the shape of the impactor to allow for verification of the assumptions made in respect of sharp-edge impacts,
- modification of the impact angle, in order to be consistent with the phenomenological model.

The test stand was designed and constructed from scratch for the purposes of this research. The design in Catia V5 and manufacturing was carried out in-house. The basic load-bearing element of the stand was a frame welded from extruded steel angles, 10 mm thick and painted with a varnish to protect the construction from corrosion. In this element, interfaces were prepared for mounting the auxiliary tank, support profiles for the barrel and brackets holding the specimen at the proper angle.

The barrel was a honed 32H8x42 cylinder tube, made of high strength structural steel. Its length was 1m., attached by steel clamps to transverse beams, which were bolted to the frame of the stand. At one end, which was the exit of the barrel, the tube is bare, while at the other end the tube had a clamped sealing ring, connected to a diameter reducer. A 19-litre air storage tank was used as an energy source with a pressure not exceeding 10 bar. The tank had a 1/4” inlet connection and a 1 1/2” outlet connection. A manometer was also installed to control the pressure inside. The tank was supplied directly from an external source – an electric piston compressor with a maximum pressure of 8 bar. The

system was controlled by a 5/2 pneumatic valve, monostable, manually operated by a lever, and the actuator was a double toggle type actuator controlling a ball valve.

The stand was equipped with a pair of remote IR beam interruption sensors – LED 5 mm. These were used to measure the velocity of the projectile as it leaved the barrel. Due to the short distance of the sample from the barrel exit, this velocity was treated as the impact velocity. The beam break sensors were hooked up to an Adafruit Feather M0 Pro-to 32-bit computer, and a 128×32 px OLED display was responsible for the velocity display. The entire measurement system was mounted in a 3D printed housing made of polypropylene.

The specimen was mounted on an auxiliary frame with a bed, the principle of which allowed adjustment of any angle in the transverse plane in relation to the axis of impact of the projectile. The range of adjustment was from 8° to 90° and the whole was made of 4mm thick steel. A fragment of the frame and bed with the mounted specimen is shown in Figure 7.

The sample mounting area and the projectile exit from the barrel were protected by a wooden box, which protected the surroundings from the projectile reflected from the sample. In addition, the case inside was protected by rubber mats designed to stop the projectile from hitting the rear wall.

The principle of the stand was to impart energy to the striking element as a result of a sudden supply of pressure to the chamber between the projectile and the beginning of the barrel.

In order to ensure reproducible results and at the same time that each time the impact takes place by means of an edge, a special shape of the impacting element has been developed as shown in Figure 7. The wider diameter is responsible for the guidance in the barrel, while the part with the smaller diameter is responsible for the direct contact during the impact. This construction of the projectile makes it possible to change the striking part while keeping the guiding core.

In order to verify the impact resistance of the shields, tests were carried out on a test rig prepared by the company.

The process started with levelling the machine and verifying the effective operation of all valves. The next step was to adjust the auxiliary frame that holds the specimen to set an impact angle of $\alpha = 8^\circ$, according to the phenomenological model. Then, after mounting the test sample in the test stand and loading the projectile, the pressure in the main tank required to fire the projectile at the appropriate velocity, i.e. 60 m/s, was determined

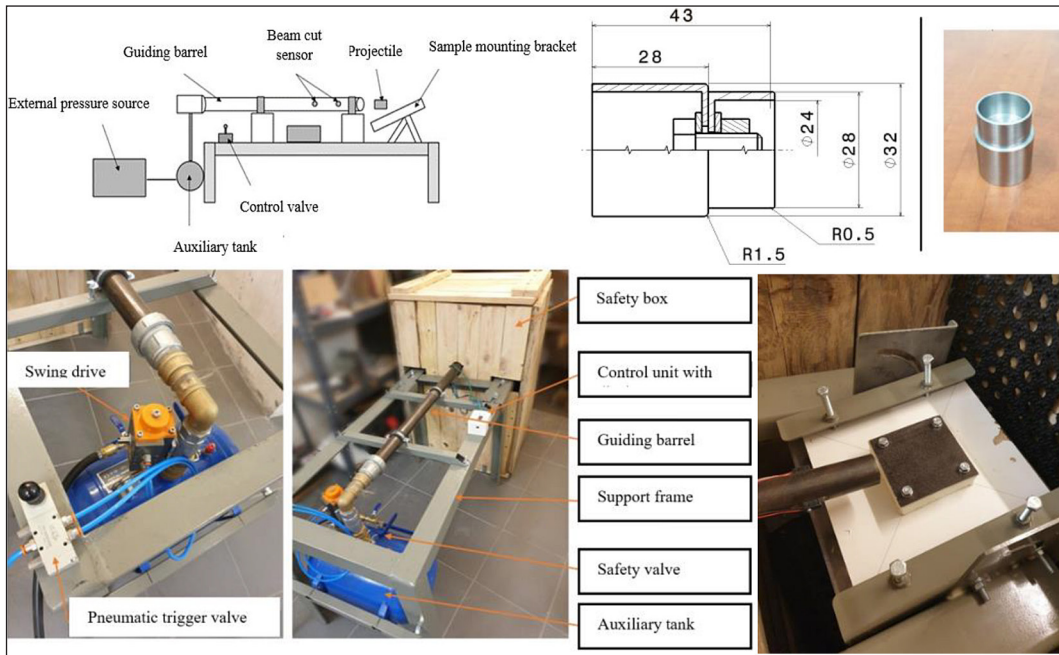


Figure 7. The striking element used in the work. On the left a cross-section of the element with dimensions, on the right the actual object

by testing. The mounted sample in the test bench is shown in Figure 8.

The set pressure required to achieve the appropriate impact energy was 3.5 bar. In order to ensure repeatability of results this value was set on the compressor regulator supplying the system. Nevertheless, during the tests it was found necessary to calibrate the test stand every 8 shots. The ambient temperature during the tests was +20 °C.

MATERIAL SAMPLES FOR TESTING

The next step in the research was to physically prepare the samples for testing. They were made of directional fabrics made of FlaxDry UD180 flax fibre, and the epoxy resin “R&G epoxy resin L”, with hardener GL2 used as a matrix. The parameters of the resin mixture are presented in Table 1. The resultant properties of the plastic formed by combining the above-mentioned flax fibres and resin

Table 1. Properties of the matrix material

Parameter	Unit	Value
Density	g/cm ³	1.2
Tensile strength	MPa	74.8
Elongation at break	%	4.5
Young's modulus	MPa	3057.0
Bending strength	MPa	119.0

mixture are presented in Table 2. The specimens consist of 6 layers of reinforcement in the following arrangement: [0, +20, -20, -70, 90, +60].

The lamination method used was vacuum resin infusion, a development of the vacuum bag method. Composite material is in accordance with the fibre direction in the respective outer layers. Efficient resin flow was ensured by a perforated foil infusion grid. Each sample was described in the form of a three-digit coding X1.X2.X3, where X1 denotes the number of the vacuum bag in which the panel was located, X2 denotes the number of the panel in a given bag, X3 specifies the number of the sample in the panel. The numbering is important because the samples from the vacuum bag X1=1 and X1=2 are characterised by a higher roughness of the outer layer and thus a higher coefficient of friction, which was used in the later bench tests. Samples from bag X1=3 and X1=4 have a smooth outer surface.

The whole process of sample creation was divided into stages, during the first hour the composite was deaerated with heating up to 30 deg, then the composite was supersaturated without heating. The next step was to stabilise the vacuum at 0.6 bar and to maintain this state for 24 hours at 17 deg [41].

After disconnecting the vacuum, the waiting time before demoulding was 24 hours. Due to the fact that lamination of natural fibres is rare, some interesting phenomena and deviations from standard

Table 2. Parameters of the composite laminate obtained after combining flax fibres and resin mixture

Parameter	Symbol	Unit	Value
Density	ρ	kg/m ³	1225.0
Young's modulus longitudinal	E1	GPa	35.0
Young's modulus transversal	E2	GPa	4.7
Young's modulus perpendicular	E3	GPa	4.7
Modulus of elastic deformation	G12	GPa	4.5
Longitudinal compressive strength	XC	MPa	318.0
Longitudinal tensile strength	XT	MPa	1791.1
Transverse compressive strength	YC	MPa	158.9
Transverse tensile strength	YT	MPa	22.6
Shear strength	SC	MPa	71.8

procedures were observed, such as the inability to heat the composites during resin suction and curing, due to boiling of water particles absorbed in the flax fibres. Another challenge was the need to lower the vacuum after resin aspiration in order to achieve low porosity.

A single specimen has dimensions of 120 × 120 mm +/- 0.8 mm and a thickness of 2.1 mm. Mounting holes were made in the corners of the specimens. These holes made it possible to connect the specimens to the foam core and to subsequently embed and fix the specimens in the test rig.

Each laminated specimen was bonded with a layer providing appropriate stiffness. For this purpose, two commercially available materials were used, i.e. expanded polystyrene EPS80 and extruded polystyrene XPS, with properties described in Table 3. The values of Young's modulus were read from the graph of modulus versus material density, presented in detail in the article [42].

Due to technological limitations and the need for freedom in the selection of proper material parameters, the core was not glued permanently to the laminate, but the specimens were screwed on the test stand to the holding interface. Details of the assembly can be seen in Figure 8. In order to avoid deformation of the specimen during twisting, each screw was tightened to an appropriate torque value, i.e. 15 Nm using a torque spanner. The laminated specimen with a filler layer is shown in Figure 8.

The factor, denoted as 'a', in Table 4 determines:

- a = 0: low coefficient of friction,
- a = 1: high coefficient of friction.

The factor, denoted as 'b', determines the direction of impact relative to the direction of greatest stiffness of the layers to be damaged. It is denoted as follows:

Table 3. Parameters of plastics used for the core

Parameter	Unit	EPS80	XPS
Density	kg/m ³	15	35
Young's modulus	MPa	3	11

- b= 0: $\beta = 0^\circ$,
- b= 1: $\beta = 90^\circ$.

The angle β is shown in Figure 10. In the case presented, the angle is 90° therefore corresponding to variant b1. The last factor determines the ability of the material to damp the impact energy and is denoted as "c". It is divided according to the value of the coefficient of restitution which characterises the respective groups of specimens. The determination of their values is presented as:

- c = 0: lower restitution factor,
- c = 1: higher restitution factor.

In order to carry out bench tests to determine the coefficient of restitution, the previously prepared 24



Figure 8. Composite sample with XPS core

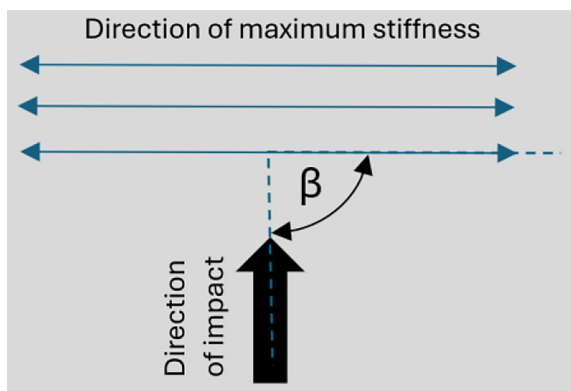


Figure 9. Representation of the angle β defining the main direction of the stiffness of the interior layers of the specimen relative to the direction of impact, in this case $\beta = 90^\circ$

specimens were divided according to the type of core which impairs the sandwich structure. The specimens were divided into 2 groups according to the nomenclature:

- **0 - EPS80 core,
- **1 - XPS core.

MEASUREMENT OF THE COEFFICIENT OF RESTITUTION

In order to verify the influence of a material’s ability to damp energy on its resistance to angular impacts, it was necessary to determine the coefficient describing the material’s spring and damping properties. This can be done in a number of ways, one of which is to experimentally determine the restitution factor “R” and from this determine the damping coefficient (Fig. 10). The effectiveness of this method has been reported by Khatami, Seyed Mohammad, et al [29].

The graph representing the values of the restitution coefficient for the samples of group **0 showed a high symmetry and closeness to the median: 0.693

to the arithmetic mean value: 0.692. The situation was different in group **1, where the mean value: 0.749 (grey line inside the blue box) was away from the median: 0.740. The interval, represented on the graph by the horizontal segments enclosing the box plot, for group **1 took the value of 0.022, indicating a relatively wide range of results.

Based on the above information, the percentage difference between the averages of the two groups of samples was calculated to be approximately 7%.

In order to statistically verify the significance of the results, a Student’s t-test was performed, which confirmed the significance of the differences between the two studied groups of samples at the level of $p < 0.001$. This confirmed the significant influence of the type of core used on the value of the restitution coefficient. The values of the restitution factor adopted for the simulations are shown in Table 5.

RESULTS FROM IMPULSE IMPACT VERIFICATION TEST BENCH

Prior to testing, the test stand was levelled and calibrated using a ceramic sample with the parameters specified in the standard [28]. After a successful calibration process, bench testing of the target specimens began. In order to minimise the measurement error and the possible influence of external factors, each of the 24 samples was verified three times.

The size of each damage was determined by measuring its area and depth. The depth of the damage was measured using a dial indicator and represented the maximum measured value.

Hence, the volume calculated from this is the theoretical volume, which is used to compare damage areas between samples and trials and to perform statistical analyses.

In order to visualise the results, one example of a damaged sample from each variant is presented (Fig.11), while a quantitative description of all

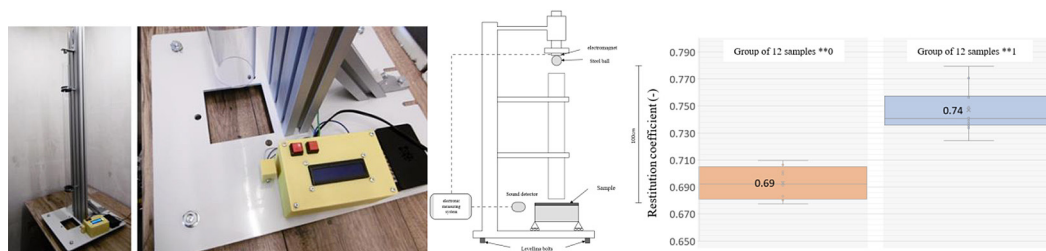


Figure 10. Schematic of test rig for determining the coefficient of restitution and box plot showing the distribution of restitution factor measurements for 24 samples. Noticeable the division into 2 groups according to the type of core (**0, **1)

Table 4. Quantitative description of laboratory test results in terms of lesion size and depth

Lp.	Designation code samples	Surface damage (mm ²)	Depth damage (mm)	Volume damage (mm ³)
1	000	111.0	0.1	11.1
2	000	221.0	0.2	44.2
3	000	187.0	0.2	37.4
4	001	2459.0	Destruction	-
5	001	744.0	0.4	297.6
6	001	363.0	0.7	254.1
7	010	236.0	0.5	118.0
8	010	186.0	0.4	74.4
9	010	231.0	0.4	92.4
10	011	997.0	0.4	398.8
11	011	1761.0	2.1	3698.1
12	011	391.0	1.3	508.3
13	100	300.0	0.2	60.0
14	100	486.0	0.2	97.2
15	100	380.0	0.5	190.0
16	101	1327.0	0.3	398.1
17	101	1087.0	1.5	1630.5
18	101	386.0	1.2	463.2
19	110	512.0	0.4	204.8
20	110	450.0	0.4	180.0
21	110	521.0	0.4	208.4
22	111	2251.0	2.1	4727.1
23	111	675.0	0.5	337.5
24	111	503.0	0.3	150.9

Table 5. Restitution factor ‘R’ values for both groups of samples

Parameter	The value of the “R” factor
Sample group **0	0.69
Sample group **1	0.74

samples in the form of the results of measurements of the resulting damage is presented in Table 4.

IMPACT OF THE RESTITUTION COEFFICIENT FACTOR ON RESULTS

The samples were prepared and sorted according to the guidelines resulting from the experiment plan described earlier, and a total of 24 composite plates were tested. Each of the 8 variants of samples with different combinations of “a”, “b”, “c” factor values were prepared in 3 pieces. The samples were then evenly distributed in 3 blocks so that within one block all variants were tested one at a time. Each

block meant one series of bench tests. In order to eliminate the influence of potential heterogeneity of sample material, samples from different panels were directed to each test.

Based on the analysis of damage occurring on the tested samples, preliminary conclusions were drawn concerning the relationship between the occurrence of the relevant factor and the shield resistance to damage of outer layers.

The analysis of results presented in Table 4 allowed to observe a great diversity of damage ranges. Particularly noteworthy is the fact that there are variants, which fundamentally differ in results within the same type of samples. This indicates the occurrence of additional, independent external factors that cannot be seen during the tests. These include e.g. a slight deviation of the projectile axis in relation to the sample, resulting from the fact that the barrel is not threaded, which may cause the projectile to be misaligned.

The additional movements of the projectile during the flight can be taken into account. As another independent factor, small differences in projectile velocity or minimal differences resulting from

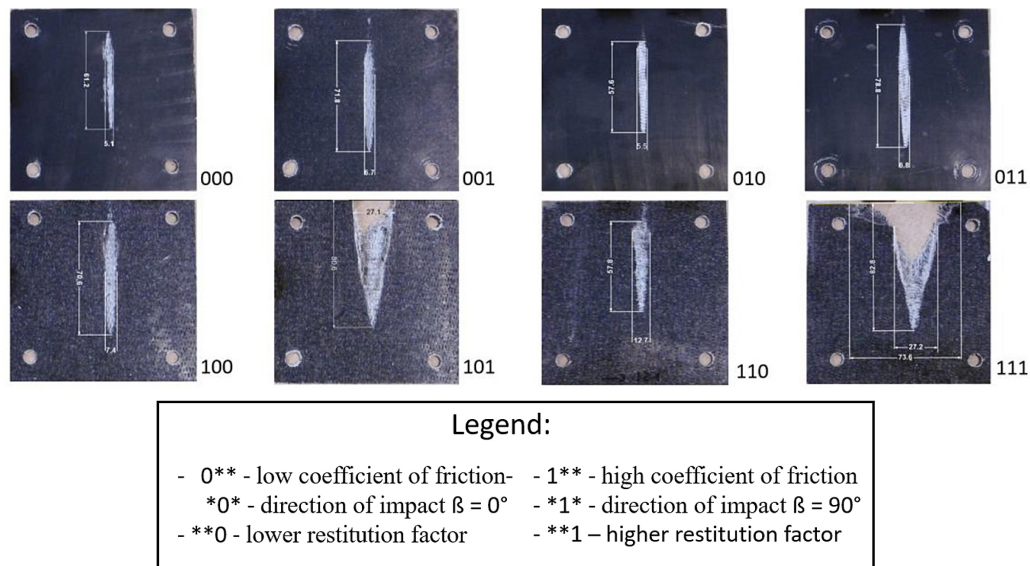


Figure 11. Samples from all groups after impact

the position of the specimens after disassembly and assembly of the next piece in the test stand, resulting from manufacturing tolerances of the elements, can be assumed. Repeatability of results for samples from groups 000, 010, 100 and 110 proves their low sensitivity to external factors, samples within the presented groups present very similar damage areas. All of the mentioned samples are based on a core with a lower restitution factor, which allows the conclusion that the type of core influences not only the extent of the damage, but also sensitivity to external factors. In the case of a core with a higher restitution factor, a small change in the conditions causes a significant increase in the extent of the damage. This is evidenced by the occurrence in each case of at least one sample in which the laminate was not completely perforated and another which was completely degraded.

In the case of one specimen, designation 001, there was a crack propagating from the axis of impact of the projectile and passing through the axes of the mounting holes, which disqualified the specimen due to complete destruction. There was probably a material defect that contributed to this type of damage.

The damage observed in samples of groups 101 and 111, an example of which is presented in Figure 11, is slightly different. These samples are based on a rigid core and have a higher friction coefficient. In this case, a damage shape resembling the letter “V” can be observed, and moreover, in the case of both samples, complete penetration occurred in the final part. This variation in results may come from differences in material quality. Indeed, in the case of laminated composite materials, there is no repeatability known from materials such as metal.

The analysis of damage depths made it possible to select variants with the greatest damage deep into the material. Without taking into account cases of total destruction, the greatest depths were observed in the case of damage to samples from groups 001, 011 and 111. On this basis it may be assumed that such a combination of parameters results in the greatest depth of penetration. All variants share the same core type, but differ in friction coefficient and impact angle.

For samples from groups 000, 010 and 110, a high convergence of results was observed, confirming that samples with a core with a lower restitution factor are less exposed to unintentional external factors. In addition, measuring the depth of the samples showed that the smallest measured depth of damage occurred for sample 000 and was 0.1 mm. Together with the smallest depth, samples of this group also have the smallest areas of damage, which proves that the system of factors characterising this group of samples provides the best resistance to the considered impacts. The average damage volumes for each group of samples were calculated from Table 4. These values were used for comparisons of the resulting damage, distinguishing between factors.

IMPACT OF THE FRICTION COEFFICIENT ON RESULTS

When considering the effect of the friction coefficient on the extent of damage, one can see its significant influence on the results. The result of the analysis of volumes observed in respective, analogous variants differing in friction factor values,

with the same values of the other coefficients, is presented in Tab.6. The magnitude of the effect depends on the presence of the other factors, but for all combinations, the damage is less for the variant with the lower friction coefficient. The biggest difference was observed between samples from group 000 and 100, in this case the average damage volume observed in samples from group 000 is 73% smaller than the average damage volume of samples from group 100. This proves the biggest influence of changing the friction coefficient value when the impact is in the direction consistent with the direction of the greatest stiffness of the layers undergoing damage and with a lower restitution coefficient.

These observations coincide with studies on the effect of friction coefficient value on the extent of damage described in conference materials [16].

IMPACT OF THE FIBRE DIRECTION ON RESULTS

The extent of the influence of the fibre direction in the outer layer relative to the impact direction was determined by analogous comparison of the mean damage volumes calculated for each group of specimens, as was done for friction. The comparison involved pairs of groups of specimens with varying values of the impact angle “ β ” while keeping the other factors the same.

Based on the analysis of data from Table 6, it can be stated that the damage area increases for specimens with the direction of the highest stiffness of damaged layers perpendicular to the impact direction ($\beta = 90^\circ$). The highest difference was observed for the pair of specimen groups 001 and 011. The average damage volume of specimen from group 001 is 82% smaller than the average damage volume of specimen from group 011. Both groups of specimens have in common a low value of the friction coefficient and a higher value of the restitution coefficient.

Furthermore, the observation of the damage area for an angle $\beta = 90^\circ$, in some cases, showed the occurrence of the phenomenon of tearing of resin fragments by overstretched transverse fibres. In addition to this, ripping and shearing of fibres contributed to an increased damage area. The phenomenon of differentiated damage levels for both cases was described in detail by Friedrich et al. [34], while a detailed discussion on this subject is described in [38]. An extended issue of the influence of e.g. core stiffness on the energy consumption of shields is described in his works by Kolenda [7], and experimental

research on this subject has been conducted and published, among others, in publications [43–44].

CONCLUSIONS

The analysis was based on a theoretical parameter defined as “Damage volume”, which is the product of the damage depth and area, the values of which are presented in Table 4. On its basis, a statistical test of the effect of the significance of individual main effects and interactions on the results was performed. For this purpose, a preliminary analysis of variance was first performed for a $2 \times 2 \times 2$ experiment set up using the completely randomised block method.

The conducted research and the obtained results made it possible to define valuable suggestions for the constructors of protective casings for the undercarriages of rail vehicles. Based on the analysis of the experimental results, the influence of factors such as the restitution coefficient, the direction of the impact relative to the direction of the fibres in the outer layers, and the friction coefficient on the extent of damage is shown. On this basis, general suggestions for designers to increase the resistance of shields to damage are as follow:

1. The shield to be constructed shall have the lowest possible value of the coefficient of restitution “R”.
2. The direction of maximum stiffness of the material should coincide with the direction of impact. This can be ensured by using directional fibres and arranging them in the outer layers of the composite in the direction of vehicle movement, bearing in mind that the minimum required lateral stiffness must also be ensured.
3. The value of the coefficient of friction should be reduced as far as possible to allow the stone to slip during impact.

The analysis of damages from tests, contributed to drawing conclusions regarding the requirements for the casing. In particular, the unidirectional nature of the damage proved to be important, which drew attention to the possibility of using the anisotropy of composite materials.

The use of composite materials for securing the chassis of new vehicles seems to be the right solution. Despite the fact that many various strength properties have to be taken into account in the design of these materials, they also offer a number of advantages, including low weight and the favourable. The observed directional nature of damage to composite panels allows the anisotropy of composite

materials to be used to increase resistance in the direction of impact. This gives rise to the conclusion that directional fabrics should be used for the construction of composite shields. Also are important the stiffness-to-weight ratio, sound absorption and thermal insulation properties.

It has been shown that a small increase in the restitution factor of a composite, causes an undoubted increase in susceptibility to the formation of extensive damage, or even complete destruction of the sample. Moreover, an increasing value of the “R” factor also increases the diversity of results obtained in state tests. This phenomenon was not observed for samples with lower restitution coefficient, the results between series were very similar to each other.

To develop an FE model to represent the low angle impact phenomenon and obtain results similar to those of bench tests, it is necessary to tune the model on the basis of experimental results. However, it is possible to further use the same model to run simulations with changed parameters for which bench testing is impossible or uneconomical for various reasons.

The advantage of numerical tests over the results of experimental studies are in the ease of observing the damage in every single layer of the composite. Observations from experimental tests do not allow for an accurate verification of damage at the layer boundary without additional, complicated analyses. In the case of the numerical model, there is a possibility of easy verification. The results from FEM simulations will show the projectile damages of the the plate in two ways: by direct impact of the striking element on the specimen which causes damage in the outer layers, and by indirect action of the force which is transferred between the layers. The latter phenomenon causes damage also to layers that are not in direct contact with the penetrator, but cause considerable damage to them. Plan for further research is a study of the effect of applying an additional external coating in the form of a sprayed-on anti-gravel primer. Unfortunately, this coating will cause an unfavourable increase in the coefficient of friction, but on the other hand, it is an additional layer which can cause a part of the energy of the striking element to be lost.

REFERENCES

1. Ma D., Manes A., Amico SC., Giglio M. Ballistic strain-rate-dependent material modelling of glass-fibre woven composite based on the prediction of a

meso- heterogeneous approach. *Composite Structures*, 2019; 216: 187–200.

2. Phadnis VA., Pandya KS., Naik NK., Roy A., Silberschmidt VV. Ballistic damage in hybrid composite laminates. *Journal of Physics: Conference Series*, 2015; 628, 012092. iOP Publishing.
3. Gellert EP., Cimpoeru SJ., Woodward RL. A study of the effect of target thickness on the ballistic perforation of glass-fibre-reinforced plastic composites. *International Journal of Impact Engineering*, 2000; 24(5): 445–456.
4. Abrate S. *Impact on composite structures*. Cambridge University Press, 2005.
5. Lopes CS., Sádaba SS., Camanho PP., González C. Advanced simulation of low velocity impact on fibre reinforced laminates. 4th International Conference on Impact Loading of Lightweight Structures (ICCILS 2014), at Cape Town, South Africa, 2014.
6. Heimbs S., Heller S., Middendorf P. Simulation of low velocity impact on composite plates with compressive preload. *Proceedings of The 7th German LSDYNA Forum*, 2008.
7. Kolenda J. Positions for testing energy consumption of shields. *Zeszyty Naukowe Akademii Marynarki Wojennej*, 2009; 50: 33–40.
8. Bełzowski A., Rechul Z., Stasięńko J. Influence of low-energy impact damage on the strength of fabric-reinforced laminate. *Diagnostics*, 2004; 30.
9. Sakly A., Laksimi A., Kebir H., Benmedakhen S. Experimental and modelling study of low velocity impacts on composite sandwich structures for railway applications. *Engineering Failure Analysis*, 2016; 68: 22–31.
10. Onder A., O'Neill C., Robinson M. Flying ballast resistance for composite materials in railway vehicle carbody shells. *Transportation Research Procedia*, 2016; 14: 595–604.
11. Rachik M., Cheng P., Laksimi A. Ballast impact effect on fatigue resistance of composite based carbodyshells in railways.
12. Hou Y., Tie Y., Li Ch., Meng L., Sapanathan T., On the damage mechanism of high-speed ballast impact and compression after impact for CFRP laminates, *Composite Structures* 2019; 229: 111435.
13. Onder A., Robinson M., Harmonised method for impact resistance requirements of E-glass fibre/unsaturated polyester resin composite railway car bodies, *Thin-Walled Structures* 2018; 131: 151–164.
14. Juzun M. Influence of selected method to estimate composite material elasticity properties on results of finite element analysis. *Compos. Theory Pract*, 2019; 19: 34–39.
15. Juzun M., Cholewa W. Recommendation for the design of composite covers which protect the chassis of a rail vehicle. *Vibrations in Physical Systems*

- 2020; 31: 2020107.
16. Juzun M., Pawlak M. Influence of impact angle and coefficient of friction on high velocity polymer composite damage. 4th International MERGE Technologies Conference IMTC 2019 Lightweight Structures, pages 2019; 119–120.
 17. Afnor: NF F07-101 Railway applications - shock test by throwing up ballast simulation. 2006.
 18. Saeedi A., Motavalli M., Shahverdi M., Recent advancements in the applications of fiber-reinforced polymer structures in railway industry – A review, *Polymer Composites*. 2024; 45: 77–97.
 19. Kalinowski M., Szczepanik M., Szymiczek M., Flammability and Mechanical Testing of Sandwich Composite for Rolling Stock Structural Applications, *Materials* 2024; 17: 5125.
 20. Esveld C. Modern railway track, volume 385. MRT-productions Zaltbommel, Netherlands, 2001.
 21. Esveld C. Recent developments in slab track. *European railway review* 2003; 9(2): 81–85.
 22. Gautier P-E. Slab track: Review of existing systems and optimization potentials including very high speed. *Construction and Building Materials* 2015; 92: 9–15.
 23. Jing G., Ding D., Liu X. High-speed railway ballast flight mechanism analysis and risk management-a literature review. *Construction and Building Materials*, 2019; 223: 629- 642.
 24. Kurpanik K., Sebastian S., Machoczek T., Woźniak A., Duda S., Kciuk S., Assessment of the Conveyor Belt Strength Decrease due to the Long Term Exploitation in Harmful Conditions, *Advances in Science and Technology Research Journal* 2024; 18(4): 1–11.
 25. Quinn A-D., Hayward M., Baker C-J., Schmid F., Priest J-A., Powrie W. A full- scale experimental and modelling study of ballast flight under high-speed trains. *Proceedings of the Institution of Mechanical Engineers, Part F: Journal of Rail and Rapid Transit*, 2010; 224(2): 61–74.
 26. Saat M-R., Jacobini F., Tutumluer E., Barkan CPL. Identification of high-speed rail ballast flight risk factors and risk mitigation strategies. Institute report, 2015.
 27. Iikura S., Kawashima K., Endo T., Fujii T. Evaluation of snow accretions under the car body using the digital pictures. *RTRI report*, 2002; 16(8): 47–52.
 28. Kawashima K., Iikura S., Endo T., Fujii T. Experimental studies on ballast-flying phenomenon caused by dropping of accreted snow/ice from high-speed trains. *RTRI Reports*, 2003; 17(8): 31–36.
 29. Khatami SM., Naderpour H., Barros RC, Jakubczyk-Gańczyńska A., Jankowski R. Effective formula for impact damping ratio for simulation of earthquake-induced structural pounding. *Geosciences*, 2019; 9(8): 347.
 30. International Organization for Standardization: 10545-5. Ceramic tiles-part 5: Determination of impact resistance by measurement of coefficient of restitution. BSI Standards Ltd, 1998.
 31. Anagnostopoulos S.A. Pounding of buildings in series during earthquakes. *Earthquake engineering & structural dynamics*, 1988; 16(3): 443–456.
 32. Marinack MC., Musgrave RE., Higgs III CF. Experimental investigations on the coefficient of restitution of single particles. *Tribology Transactions*, 2013; 56(4): 572–580.
 33. Patil D., Higgs C-F. A coefficient of restitution model for sphere-plate elastoplastic impact with flexural vibrations. *Nonlinear Dynamics*, 2017; 88(3): 1817–1832.
 34. Friedrich K., Varadi K., Goda T., Giertzsch H. Finite element analysis of a polymer composite subjected to a sliding steel asperity part ii: Parallel and anti-parallel fibre orientations. *Journal of materials science*, 2002; 37(16): 3497–3507.
 35. Brzezinski J. Methodology of psychological research. PWN Scientific Publishers, 2019.
 36. Królikowski W. Polimerowe kompozyty konstrukcyjne. Wydawnictwo Naukowe PWN Warszawa, Poland, 2012.
 37. ASTM International: Standard Test Method for Measuring the Damage Resistance of a Fiber-reinforced Polymer Matrix Composite to a Drop-weight Impact Event. ASTM International, 2007.
 38. Mzali S., Elwasli F., Mkaddem A., Mezlini S. FE modelling of wear mechanisms in ud-gfrp composites using single-indenter scratch test: A micromechanical approach. *Advances in Acoustics and Vibration*, Springer, 2017; 269–279.
 39. International Organization for Standardization: 20567-1:2017 Paints and varnishes - determination of stone-chip resistance of coatings - part 1: Multi-impact testing. 2017.
 40. ASTM International: D7136/d7136m, measuring the damage resistance of a fiber- reinforced polymer matrix composite to a drop-weight impact event.
 41. RG Composite Technologies. Report for the Silesian University of Technology 01/01.
 42. Bartlett SF., Neupane R. Seismic evaluation of expanded polystyrene (eps) geofoam bridge support system for overpass structures. Institute report, 2017.
 43. Rybak P., Borkowski W., Michałowski B., Hryciów Z. Testing of protective casings of special vehicles. X Conference “FEM programs in support of analysis, design and manufacturing”, 2007; 13–16.
 44. Ochelski S., Bogusz P., Michałowski B., Hryciów Z. Energy absorption capacity of various structures of energy-intensive structures. X Conference “FEM programs in support of analysis, design and manufacturing”, 2007; 13–16.